CHAPTER 15

Biosensors for the Detection of Calcium and pH

Paolo Pinton, Alessandro Rimessi, Anna Romagnoli, Andrea Prandini, and Rosario Rizzuto

Department of Experimental and Diagnostic Medicine, Section of General Pathology
Interdisciplinary Center for the Study of Inflammation (ICSI) and
Emilia Romagna Laboratory for Genomics and Biotechnology (ER-Gentech)
University of Ferrara, I-44100 Ferrara, Italy

I. Introduction

The development of diverse molecular biology techniques, which can modify and express exogenous cDNAs in virtually all cell types, has been responsible for the recent expansion in the use of protein probes for imaging studies in cell biology. Two groups of visualizable reporter proteins are currently employed: the chemiluminescent proteins

METHODS IN CELL BIOLOGY, VOL. 80

0091-679X/07 $35.00
DOI: 10.1016/S0091-679X(06)80015-4

(e.g., aequorin from *Aequorea victoria* and luciferase from *Photinus pyralis*), and the fluorescent proteins (e.g., green fluorescent protein [GFP] from *A. victoria* and red fluorescent protein [DsRFP] from *Discosoma* sp.).

The study of isolated mitochondria, dating back to the 1960s, has provided a wealth of information on the biochemical routes that allow these organelles, derived from the adaptation of primordial symbionts, to couple oxidation of substrates to the production of ATP. Moreover, recent work has highlighted the role of signals reaching the mitochondria in the activation of apoptosis. In this context, it is an exciting task to study mitochondrial function in living cells. For this purpose, new tools are needed, that combine specific targeting to mitochondria and the sensitivity to detect the parameter of interest. Recombinant reporter proteins are emerging as the tools of choice, since their light output can be robust, and they can be targeting to compartments of interest using signal sequences.

In particular, we describe the development and use of protein chimeras (derived from proteins naturally present in the medusa, *A. victoria*) that are specifically targeted to the mitochondria, either to the matrix or to the intermembrane space and can be used to monitor calcium and pH. Aequorin, the pioneer of the targeted recombinant probes, is a Ca^{2+}-sensitive photoprotein that emits light on binding of Ca^{2+} to its three high affinity Ca^{2+}-binding sites. We also describe the use of mutants of GFP as Ca^{2+} and pH probes.

II. Targeting Strategies and Transfection

The strategy used to achieve the correct delivery of recombinant probes to mitochondria takes advantage of the naturally occurring signal peptides that are present in nuclear-encoded mitochondrial proteins (Fig. 1). The vast majority of mitochondrial proteins are encoded in nuclear DNA, synthesized in the cytosol, and imported into the organelle. Correct targeting of these nuclear-encoded mitochondrial proteins is mediated by signal peptides, which are usually present at the N-terminus. Mitochondrial signal sequences have no consensus sequence but bear some common amino acid compositions, charge distribution and in some cases, secondary structure (Gavel and von Heijne, 1990) (for details on import of proteins into mitochondria, please refer to Chapter 35 by Habib *et al.* and Chapter 36 by Stojanovski *et al.*, this volume).

A. Targeting to the Mitochondrial Matrix

Subunit VIII of human cytochrome *c* oxidase possesses a 25-amino acid signal peptide at its N-terminus, which is cleaved by the matrix protease on import. It is presumed that the action of the protease is dependent on a motif present within the first few amino acids of the mature protein (Rizzuto *et al.*, 1989). To target functional reporter probes to the mitochondrial matrix, a chimera is constructed which consists of the first 31 amino acids of COX Subunit VIII, which contains the

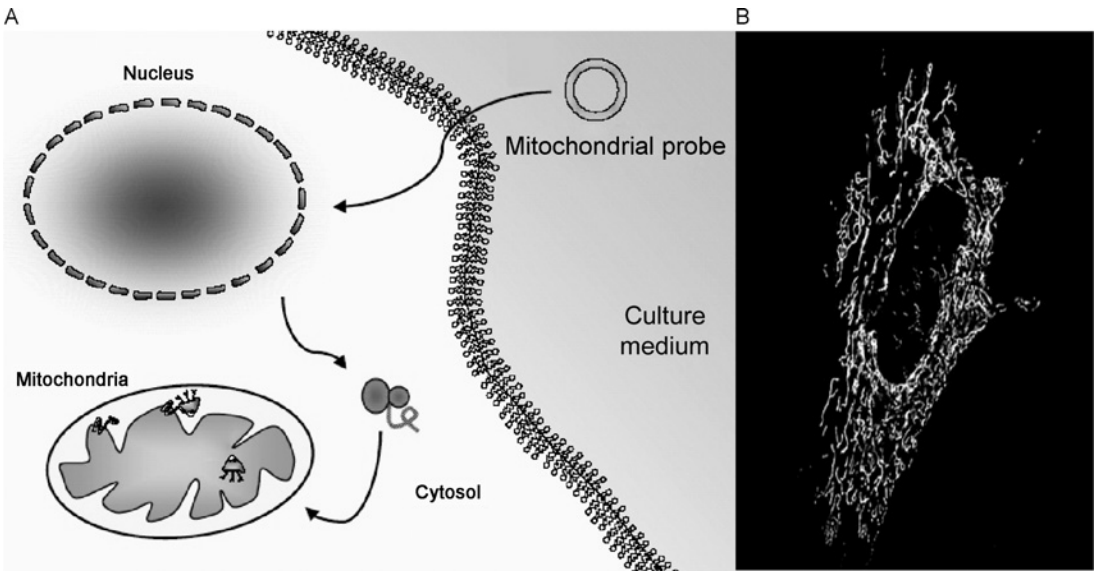

Fig. 1 Transfection of reporter constructs. (A) Recombinant expression of a mitochondrial probe. The cDNA of the reporter protein is introduced into cells by transfection. The precursor protein is synthesized by the cellular machinery and imported into mitochondria. For the mitochondrial matrix, HA1-tagged probe is fused to the cleavable-targeting sequence (mitochondrial presequence) of a subunit (e.g., VIII) of cytochrome *c* oxidase, the terminal complex of the respiratory chain. For the MIMS, the gene-encoded probe is fused to the C-terminus of GDP, an integral protein of the mitochondrial inner membrane that has a large C-terminal domain protruding into the intermembrane space. (B) Immunolocalization of mtAEQ 36 h after transfection was carried out by standard procedures.

matrix-targeting signal peptide and the first 6 amino acids of the mature protein, fused to the N-terminus of the reporter protein of interest (e.g., aequorin or GFP mutant) (De Giorgi *et al*., 1996; Rizzuto *et al*., 1992).

B. Targeting to the Mitochondrial Intermembrane Space

For the delivery of probes to the mitochondrial intermembrane space (MIMS), we exploited the characteristics of glycerol phosphate dehydrogenase (GPD), an enzyme that is integrated into the mitochondrial inner membrane with its C-terminal domain protruding into the MIMS. To target aequorin and GFP to this space, we fused the photoprotein to the C-terminal portion of GPD. This allowed for efficient targeting of the reporter protein to the intermembrane space, without altering its C-terminus, which is essential for its luminescent properties (Pinton *et al*., 1998; Porcelli *et al*., 2005; Rizzuto *et al*., 1998b). In all cases, an epitope tag (9-aa-long HA1 hemagglutinin) is added to the coding region of the reporter protein, to allow immunolocalization of the transfected protein.

Our experience has been that mitochondrial reporter constructs are sorted to the expected location efficiently and quantitatively. However, when a series of experiments is initiated in a new cell type, it is prudent, especially with photoproteins that cannot be directly visualized under the microscope, to confirm the correct sorting. Figure 1B shows the immunolocalization of one of these constructs (mitochondria-targeted aequorin, mtAEQ). The typical rod-like appearance of mitochondria can be easily appreciated.

The first step in mitochondrial measurements with recombinant reporter probes is the introduction of the encoding cDNA into the cell type of interest (Fig. 1A). Introduction of foreign DNA into cells is generally feasible using the calcium phosphate method. Certain cell types, however, are particularly resistant to this procedure. In such cases, the solution has been to seek alternative methods for the introduction of cDNA into that particular cell type. Since detailed protocols are supplied by the manufacturers of both kits and specific instrumentation, these are not be discussed in this chapter. In our experiment, we have determined empirically that all cell types in which we have tried to express chimeric probes can be transfected successfully using one method or another.

III. Calcium Reporters

The contribution of mitochondria to intracellular Ca^{2+} signaling and the role of mitochondrial Ca^{2+} uptake, both in shaping the cytoplasmic response and in controlling mitochondrial function, are currently areas of intense investigation (Bernardi, 1999; Budd and Nicholls, 1996a,b; Duchen, 2000a,b; Nicholls, 2005; Pozzan and Rizzuto, 2000; Rizzuto and Pozzan, 2006; Rizzuto *et al.*, 2000). These studies rely to a large extent on the appropriate use of emerging techniques combined with judicious data interpretation. The outer and inner mitochondrial membranes (OMMs and IMMs, respectively) are markedly different, architecturally as well as functionally. It is noteworthy that the IMM is very impermeable to ions in general, including Ca^{2+}.

Mitochondrial Ca^{2+} traffic takes place essentially through two pathways: (1) a ruthenium red (RR)-sensitive electrogenic Ca^{2+} uniporter that exhibits a very low affinity ($K_m \sim 5$–$10\ \mu M$) for the cation, allows for the transport of Ca^{2+} down its electrochemical gradient ($\sim$200 mV on the side of the matrix) and (2) an electroneutral antiporter that, by exchanging Ca^{2+} with either Na^+ or H^+, prevents the attainment of an electrochemical equilibrium (Fig. 2) (Carafoli, 1987; Gunter and Gunter, 1994, 2001; Gunter *et al.*, 2000; Pozzan *et al.*, 1994).

Although the biochemical properties of these transport pathways have been known for over three decades, the molecular events that regulate the dynamics of this transport system were not well understood. Nevertheless, a role for mitochondria in Ca^{2+} signaling is widely accepted and work was initiated to clarify the precise function of mitochondria in these signal transduction events (Berridge *et al.*, 2000, 2003; Duchen, 1999, 2000a; Hajnoczky *et al.*, 1995; Rizzuto and Pozzan, 2006;

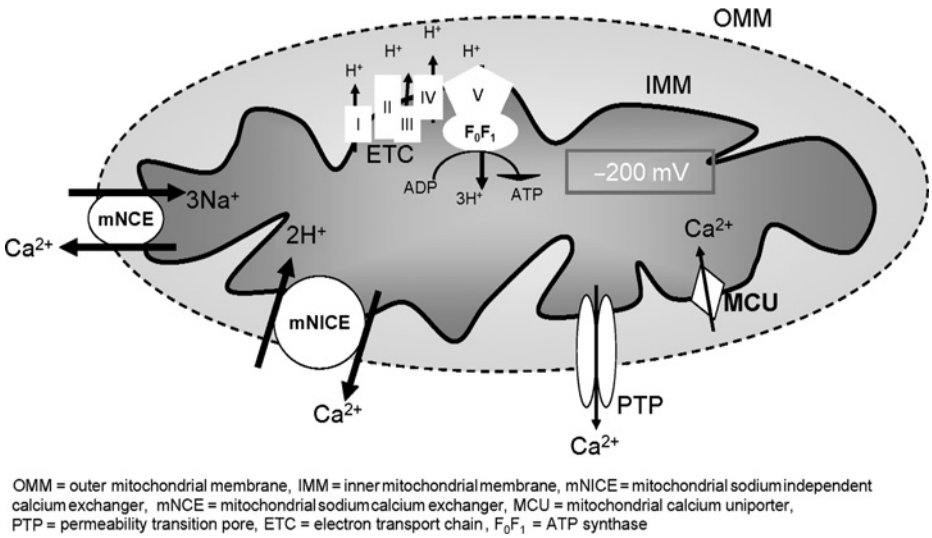

Fig. 2 Calcium trafficking in mitochondria. Ca^{2+} entry takes place via a low affinity uniporter (which is inhibited by RR), due to the high electronegative potential (which is collapsed by FCCP or CCCP) in the mitochondrial matrix. Extrusion of Ca^{2+} takes place through an electro-neutral antiporter (in exchange with either Na^+ or H^+). In the matrix, Ca^{2+} stimulates the activity of three Ca^{2+}-sensitive dehydrogenases of the Krebs cycle (NAD^+-isocitrate-, 2-oxoglutarate-, and pyruvate-dehydrogenase), thus promoting electron flow through the electron transport chain (ETC).

Rizzuto *et al.*, 2004). An obvious function for mitochondrial Ca^{2+} homeostasis was soon found, namely, to rapidly adapt aerobic metabolism to the changing needs of a cell. However, subsequent work revealed a much broader picture. It showed that mitochondrial Ca^{2+} uptake influences the kinetics and spatial properties of the cytoplasmic concentration of Ca^{2+} or $[Ca^{2+}]_c$ (Budd and Nicholls, 1996a; Drummond and Fay, 1996; Herrington *et al.*, 1996), and that within the mitochondrion a Ca^{2+}-mediated signal can induce a radically different effect, that is, triggers the onset of apoptosis (Duchen, 2000b; Green and Kroemer, 2004; Kroemer and Reed, 2000).

We describe here two methodological approaches to measure the concentration of Ca^{2+} within the mitochondrial context, that is, $[Ca^{2+}]_m$. In the first part, we focus on the use of aequorin (a luminescent protein). The second part is devoted to measurements using chimeric versions of GFP (a fluorescent protein).

A. Mitochondrial Calcium Measurements Using Aequorin

Aequorin is a 21-kda protein from various *Aequorea* species (Shimomura, 1986; Shimomura *et al.*, 1962) which, in the active form, consists of an apoprotein and a covalently bound prosthetic group (coelenterazine). When Ca^{2+} ions bind to three high-affinity sites (EF-hand type), aequorin undergoes an irreversible reaction in

which a photon is emitted (Fig. 3). The use of aequorin as a Ca^{2+} probe is based on the fact that, at $[Ca^{2+}]$ between 10^{-7} and 10^{-5} M, the concentrations normally occurring in the cytoplasm of living cells, there is a relationship between $[Ca^{2+}]$ and the fractional rate of aequorin consumption (i.e., L/L_{max}, where L_{max} is the maximal rate of light production at saturating Ca^{2+} concentrations) (Allen and Blinks, 1978; Cobbold, 1980; Ridgway and Ashley, 1967). Figure 3B shows the Ca^{2+} response curve of expressed recombinant aequorin under physiological conditions of pH, temperature, and ionic strength. It is apparent that, due to the cooperativity

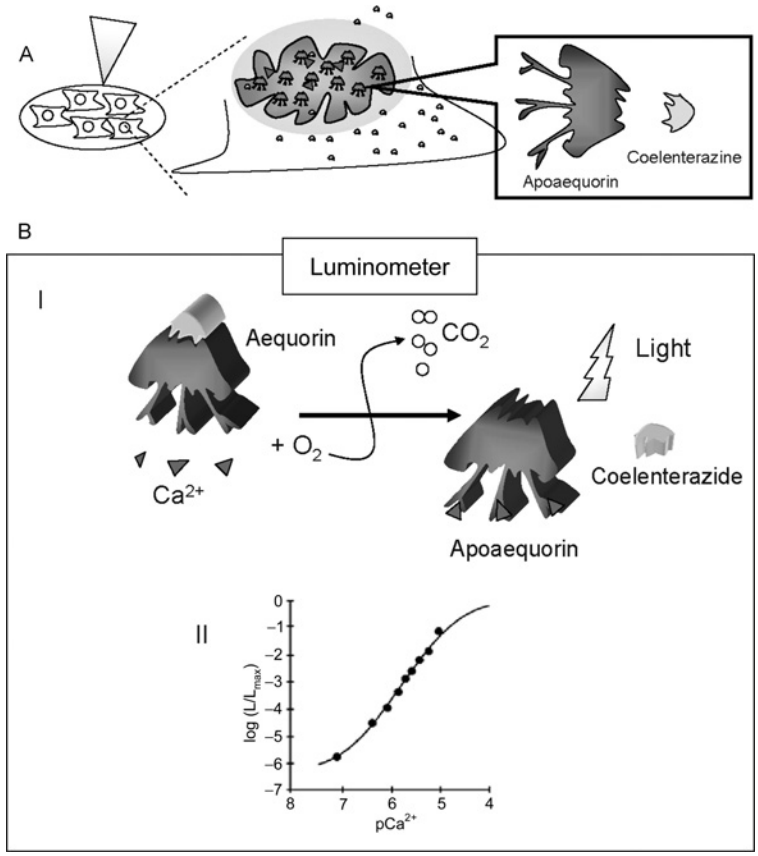

Fig. 3 Aequorin reporters. (A) Schematic representation of the Ca^{2+}-dependent photon emission in cells transfected with aequorin cDNA. The functional probe is composed of the apoaequorin moiety (synthesized by the cell) and coelenterazine (imported from the surrounding medium). (B) (I) Binding of calcium ions disrupts the binding of the prosthetic group, with concomitant light emission. (II) Relationship between calcium concentration and the rate of light emission by active aequorin (L and L_{max} are, respectively, the instant and maximal rates of light emission).

between the three binding sites, light emission is proportional to the second to third power of $[Ca^{2+}]$. This accounts for the excellent signal-to-noise ratio of aequorin. On the other, however, if the $[Ca^{2+}]$ is not homogeneous, aequorin it tends to bias the average luminosity toward the higher values (see below).

Aequorin is well suited for measuring $[Ca^{2+}]$ between 0.5 and 10 μM. However, it is possible to extend the range of measurable $[Ca^{2+}]$ by reducing the affinity of aequorin for Ca^{2+}. There are at least three different ways to reduce this affinity: (1) introducing point-mutations in the Ca^{2+}-binding sites of the apoprotein (Kendall *et al.*, 1992); (2) using surrogate cations that elicit a lower rate of photoprotein consumption than Ca^{2+}, for example, Sr^{2+} (Montero *et al.*, 1995); and (3) using modified prosthetic groups that alter the Ca^{2+}-dependent reaction. These three approaches can be combined to obtain a clear shift in the Ca^{2+} affinity of the photoprotein. Because of the cooperativity between the three Ca^{2+}-binding sites of aequorin, the aequorin mutant that we generated (Ala119 $\rightarrow$ Asp), which affects the second EF-hand domain, is suited for measuring $[Ca^{2+}]$ in the range of 10–100 μM. The range of aequorin sensitivity can be expanded further by employing divalent cations other than Ca^{2+}. We have used Sr^{2+}, a common Ca^{2+} surrogate: Sr^{2+} permeates across Ca^{2+} channels and is actively transported, although with a low affinity, by both the plasma membrane and the sarco-endoplasmic Ca^{2+} ATPases (SERCAs). By combining the two approaches, an aequorin-based ER probe can measure $[cation^{2+}]$ ranging from the μM to the mM (Montero *et al.*, 1995). To avoid possible discrepancies between the behavior of the two cations and to provide a more accurate estimate of the $[Ca^{2+}]$ in compartments with high $[Ca^{2+}]$, it is now possible to measure Ca^{2+} directly using a low-affinity coelenterazine analog (coelenterazine n) (Montero *et al.*, 1997).

While the experimental protocols will be discussed in more detail below, we will review here briefly the main advantages and disadvantages of the recombinant aequorin approach.

1. The Advantages of Aequorin

1. *Selective intracellular distribution.* The ability to engineer the protein (e.g., add highly specific-targeting sequences or introduce substitutions that alter Ca^{2+}-binding affinity) is a key advantage of genetically encoded Ca^{2+} probes, such as aequorin and fluorescent indicator based on GFP.

2. *High signal-to-noise ratio.* Due to the low luminescence background of cells and the steepness of the Ca^{2+} response curve of aequorin, minor variations in the amplitude of the agonist-induced $[Ca^{2+}]$ changes can be easily detected with aequorin.

3. *Low Ca^{2+} buffering effect.* Although the binding of Ca^{2+} by aequorin may, in principle, affect intracellular Ca^{2+} homeostasis, this undesired effect is less deleterious for aequorin compared to other fluorescent indicators. In fact, thanks to the excellent signal-to-noise ratio, aequorin is loaded at a concentration that is 2–3

orders of magnitude lower than other dyes, that is, usually from <0.1 μM (for the recombinantly expressed photoprotein) to ~ 1 μM (in the case of microinjected photoprotein for single cell studies) (Brini *et al.*, 1995).

4. *Wide dynamic range*. As is evident in Fig. 3B, aequorin can measure $[Ca^{2+}]$ accurately in the range of 0.5–10 μM, concentrations at which most fluorescent indicators are saturated. Indeed, thanks to these properties and low buffering effect, it is possible to estimate the large $[Ca^{2+}]$ rises that occur, for example, in neurons. Moreover, as described above, the range of $[Ca^{2+}]$ measurement can be increased to more than 100 μM.

5. *Possibility of coexpression with proteins of interest*. The ability to modify the molecular repertoire of a cell is one of the most powerful tools for dissecting complex, often interconnected signaling pathways. This is also true for calcium signaling, and one of the experimental tasks we often face is to measure Ca^{2+} concentrations in cells expressing a normal or mutated signaling component. It is not possible to load indicator dyes in the subset of transfected cells. Therefore, calcium measurements using indicator dyes are usually carried out using clones stably expressing the transgene (which may have altered behaviors as a result of natural variability of cell clones) or using laborious single-cell analysis of transfected cell populations. Aequorin provides an easy solution to the problem, because it can be coexpressed with the protein of interest. In transient expression studies, the Ca^{2+} probe is localized exclusively to the fraction of transfected cells (depending on the cell type), which are thus very representative of the behavior of the parental population (Bastianutto *et al.*, 1995; Lievremont *et al.*, 1997; Pinton *et al.*, 2000; Rapizzi *et al.*, 2002).

2. The Disadvantages of Aequorin

1. *Low-light emission*. The major disadvantage in the use of aequorin is the low amount of light emitted by the photoprotein. Each aequorin molecule emits only one photon, and only a small fraction of the pool of photoproteins ($<10^{-3}$) emits light throughout the experiment. This is not a major problem when light output form aequorin from an entire coverslip of transfected cells is measured, as described above. However, it is often desirable to carry out single cell-imaging experiments (e.g., to detect Ca^{2+} waves or local changes in Ca^{2+} concentration). With aequorin, such analyses are quite difficult. Special imaging systems are needed, with enhanced sensitivity at the cost of lower spatial resolution. Thus, although single cell-imaging experiments with recombinant aequorin have been carried out and have provided interesting biological information (Rutter *et al.*, 1996), this approach is technically difficult and yield low image quality.

2. *Overestimation of the average rise in cells (or compartments) with nonhomogeneous behavior*. Due to the steep Ca^{2+} response curve of aequorin, if the probe is distributed between areas of high and low $[Ca^{2+}]$, the former undergoes a much

greater emission of light. The total signal will be calibrated as an "average" [Ca^{2+}] increase that will be severely biased by the region at high Ca^{2+}. In other words, given that an increase in 1 pCa unit causes a 100 to 1000-fold increase in light emission, a tiny volume undergoing a very large increase in [Ca^{2+}] will increase total light output drastically and thus will be "interpreted" by the calibration algorithms as a moderate Ca^{2+} rise throughout the cells. Conditions can be envisaged in which this effect can become very significant. For example, a Ca^{2+} rise of 3 μM detected in neurons could be, in fact, lower, but severely biased by hotspots occurring throughout the dendritic tree.

3. *The loading procedure*. The obvious requirement of the recombinant reporter approach is that a cell must be amenable to transfection. Significant improvements in transfection techniques have made this problem less severe. In our experiment, all cell types can be transfected, with either using simple calcium phosphate procedure (which proves effective in most cell types) or using other techniques (liposomes, gene gun, electroporation). Conversely, the need to maintain the cells in culture for enough time to produce the recombinant protein can be an important limitation, rendering the extension of the approach to interesting cell types (e.g., pancreatic acinar cells, spermatozoa, and so on) quite difficult.

B. Procedure

We have employed a wide variety of cell types (e.g., HeLa, CHO, COS, neurons, myocytes) with good results in terms of aequorin expression. In all cases, the cells are seeded in coverslips (13-mm diameter) and allowed to grow until about 50% confluency. At this point, the cells are transfected with 4 μg of mtAEQ or 0.5 μg of mimsAEQ, using the calcium phosphate procedure. With mimsAEQ, we noticed that in a few cases high levels of expression had deleterious effects on the transfected cell population. This problem was solved by reducing the quantity of DNA used for transfection.

After 36 h, aequorin is reconstituted (Fig. 3A) by adding the prosthetic group to the incubation medium (5-μM coelenterazine for 2 h in DMEM supplemented with 1% FCS at 37°C in 5% CO_2 atmosphere). The cells are then washed and transferred to the perfusion chamber of the measuring system.

After reconstitution ($\sim$2 h), the coverslip is placed in the chamber of the measuring system, where it is perfused with modified Krebs-Ringer buffer saline solution (modified KRB: 125-mM NaCl, 5-mM KCl, 1-mM Na_3PO_4, 1-mM $MgSO_4$, 5.5-mM glucose, 20-mM HEPES, pH 7.4, 37°C).

The schematic representation of the measuring system is depicted in Fig. 4. In this system, the perfusion chamber, on top of a hollow cylinder (with temperature control maintained by a thermostatted by water jacket), is perfused continuously with buffer using a peristaltic pump. Agonists and drugs are added to the same KRB medium.

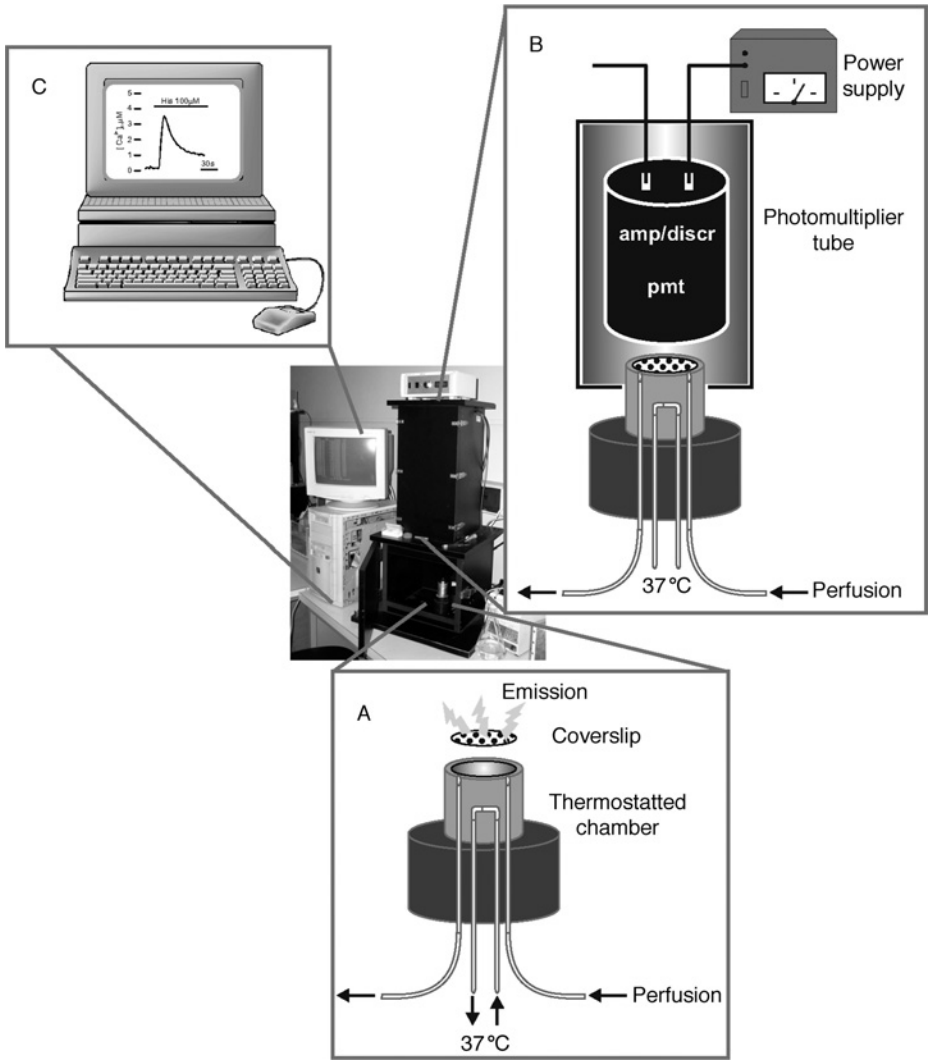

Fig. 4 Experimental setup to measure light production. (A) A thermostatted (37°C) chamber, engineered with a perfusion system, is the support for cells expressing the functional aequorin probe. Cells are plated on a coverslip which is fit into a notch positioned at the top of the chamber and then sealed with a larger coverslip. (B) The chamber is in proximity to a photomultiplier tube (pmt), with a built-in amplifier/discriminator (amp/discr) that is able to capture the light emitted in the reaction. The complete assemblage is in the dark to minimize extraneous signals. (C) An analysis system (IBM-compatible computer) records and captures the photon emission data and converts them into Ca^{2+} concentration values, using the aequorin calibration curve.

The cell coverslip is placed at few millimeter away from the surface of a low-noise phototube. The photomultiplier is kept in a dark, refrigerated box. An amplifier discriminator is built into the photomultiplier housing. The pulses generated by the discriminator are captured by a Thorn EMI photon counting board, connected to an IBM-compatible computer. The board allows the storing of the data in the computer memory for further analyses.

To calibrate the crude luminescent signal in terms of $[Ca^{2+}]$, we have developed an algorithm that takes into account the instantaneous rate of photon emission and the total number of photons that can be emitted by the aequorin in the sample (Brini *et al.*, 1995). To determine the latter, emitted light is measured in the sample, after cells used in an experiment are lyzed by perfusion with hypo-osmotic medium containing 10-mM $CaCl_2$ and detergent (100-μM digitonin). This discharges all the aequorin that was not consumed during the experiment.

1. Agonist Stimulation Causes Large and Rapid Mitochondrial Ca^{2+} Uptake in Most Cell Types

To stimulate an increase in $[Ca^{2+}]_c$, we use an agonist—histamine or ATP—that, acting on a G-protein-coupled receptor, leads to the generation of inositol 1,4,5-trisphosphate (IP_3) (Fig. 5A). Briefly, histamine or ATP (100 μM, final concentration) is added to the perfusion medium (modified KRB buffer) for 1 min, followed by rinsing in the same buffer. The biphasic kinetics of $[Ca^{2+}]_c$ in HeLa cells transfected with wild-type aequorin (without any targeting sequences and thus localized to the cytosol) is shown in Fig. 5C. The release of Ca^{2+} from intracellular stores causes an initial rapid, but transient, increase of $[Ca^{2+}]_c$ (to values of $\sim$2.5 μM), followed by a sustained increase of $[Ca^{2+}]_c$ above normal basal levels throughout the stimulation period.

Figure 5B shows the measurements obtained in HeLa cells transiently expressing mtAEQ or mtAEQmut. On stimulation with histamine, there is a rapid increase in $[Ca^{2+}]_m$ up to $\sim$10 μM (mtAEQ) or 100 μM (mtAEQmut), followed by the return, within 2 min, to almost basal values. In turn, the rise in $[Ca^{2+}]_m$ stimulates the activity of Ca^{2+}-dependent enzymes of the Krebs cycle, and hence increases mitochondrial ATP production (Jouaville *et al.*, 1999).

Similar studies can be conducted in virtually any cell type capable of being transfected. Indeed, large $[Ca^{2+}]_m$ changes were observed in a variety of cell lines and in different primary cultures (Pinton *et al.*, 1998).

2. The mimsAEQ Chimera Reveals Ca^{2+} Rises Higher Than Those of the Bulk Cytosol

The fact that alterations in $[Ca^{2+}]_m$ are much larger than those observed for $[Ca^{2+}]_c$ were unexpected, given the low affinity of the mitochondrial uniporter for Ca^{2+}. However, this apparent contradiction could be explained if the endoplasmic reticulum (ER) and the mitochondria have a close physical relationship, allowing mitochondria be exposed to microdomains of high $[Ca^{2+}]$ generate by release of Ca^{2+} from the ER (Rizzuto *et al.*, 1993, 1998b).

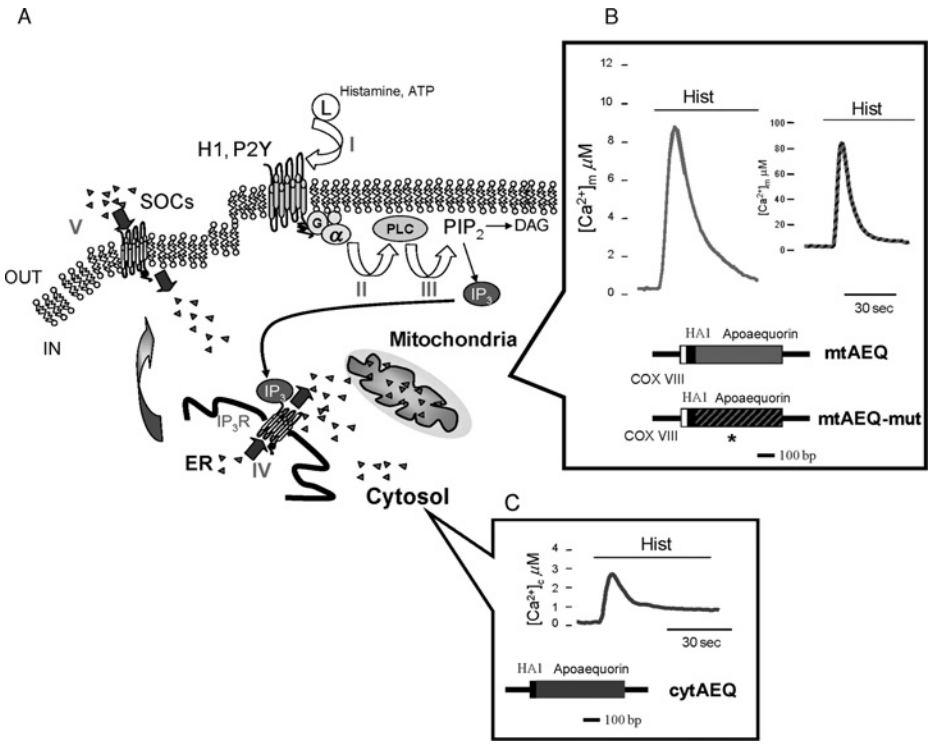

Fig. 5 Calcium measurements in mitochondria. (A) When an extracellular agonist, for example, histamine or ATP, binds to its receptor (I), a G-protein–coupled receptor is activated (II), with consequent stimulation of phospholipase C (III). Thus, phosphatidylinositol-4,5-bisphosphate is hydrolyzed to diacylglycerol and IP_3, which diffuses through the cytosol and binds to its IP_3 receptors on internal stores of Ca^{2+}. Ca^{2+} is released (IV) and an increase of $[Ca^{2+}]_c$ and $[Ca^{2+}]_m$ occurs. Emptying of the store is detected and is transmitted to the store-operated channels (SOCs) to induce Ca^{2+}-influx across the plasma membrane (V). (B) Schematic maps of the mt-AEQ-wt and -mut cDNAs. Coding and noncoding regions are represented as boxes and lines, respectively. In the coding region, the portions encoding mitochondrial targeting sequence (subunit of cytochrome *c* oxidase), the HA1 epitope (HA1) and apoaequorin are white, black and gray–gray/black, respectively. For mtAEQ-mut, the asterisk indicates a mutation in the Ca^{2+}-binding sites (Asp-119 → Ala), which causes ~20-fold decrease in the Ca^{2+} affinity of the photoprotein. Traces show the monitoring of $[Ca^{2+}]_m$ in HeLa cells transfected transiently with the probes. Where indicated, the cells were treated with 100-μM histamine (Hist), added to KRB. (C) Schematic map of the cyt-AEQ cDNA. In the coding region, the HA1 epitope (HA1) and apoaequorin are black and dark gray, respectively. The figure also includes a representative measurement showing the $[Ca^{2+}]_c$ rise evoked by histamine stimulation.

To analyze the possible existence of such high Ca^{2+} microdomains, we used a different aequorin chimera which is targeted to the mitochondrial intermembrane space (mimsAEQ). Since the OMM is freely permeable to ions and small molecules, aequorin molecules present between the two mitochondrial membranes are

located in a region that is in rapid equilibrium with the cytosolic portion in contact with the organelle. Such a chimera is thus sensitive to changes in Ca^{2+} in the cytosolic region immediately adjacent to mitochondria (Rizzuto *et al*., 1998b).

HeLa cells transfected with mimsAEQ and stimulated with histamine show a biphasic response, as shown in Fig. 6A. An initial rise in $[Ca^{2+}]_{mims}$ to ~3.5 μM is followed by a rapid decrease, that gradually levels out to values above the initial $[Ca^{2+}]$. This type of response is due to the two mechanisms of action of the agonist, namely the release of Ca^{2+} from intracellular stores and the entry of Ca^{2+} from the extracellular medium. The comparison of the responses of $[Ca^{2+}]_c$ and $[Ca^{2+}]_{mims}$ to histamine shows a clear difference only in the initial phase (the phase that is due to the release of Ca^{2+} from intracellular stores). These data support the hypothesis that the opening of IP_3-sensitive channels in the ER that are in proximity to mitochondria generate microdomains of high $[Ca^{2+}]$. Indeed, the $[Ca^{2+}]$ in such microdomains is much higher than the average $[Ca^{2+}]_c$, and thus the low affinity Ca^{2+} uptake systems present in mitochondria are capable of accumulating Ca^{2+} efficiently in the matrix of the organelle. Conversely, depletion of Ca^{2+} in the ER by a different mechanism, such as passive diffusion after blocking of the ER Ca^{2+} accumulation via ER Ca^{2+}-ATPase, caused the same rise (Fig. 6B).

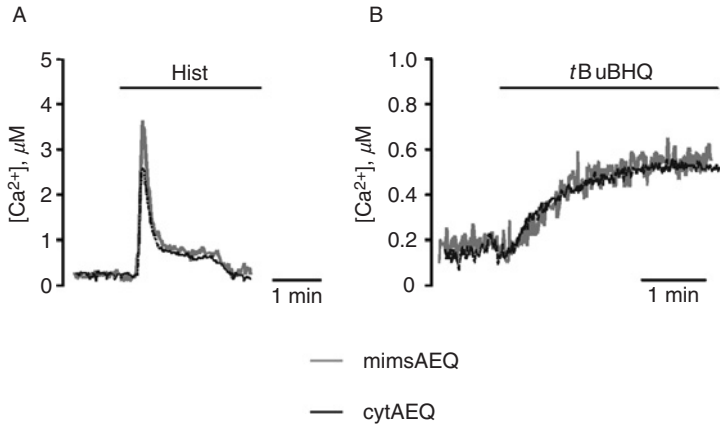

Fig. 6 Calcium measurement in the MIMS. (A) The effect of histamine on the $[Ca^{2+}]$ of the cytosol ($[Ca^{2+}]_c$) and MIMS ($[Ca^{2+}]_{mims}$). The traces show $[Ca^{2+}]$ of the two compartments in parallel batches of HeLa cells, transfected transiently with the appropriate aequorin chimera (cytAEQ or mimsAEQ). All conditions are as in Fig. 5. Where indicated, the cells were treated with 100-μM histamine (Hist), added to KRB. (B) The effect of inhibition of the sarco-endoplasmic Ca^{2+}-ATPase (SERCA) on $[Ca^{2+}]_c$ and $[Ca^{2+}]_{mims}$. All conditions are as in Fig. 5. Where indicated, the cells were challenged with 10-μM 2,5-di(*tert*-butyl)-1,4-benzohydroquinone (*t*BuBHQ), an inhibitor of the SERCAs (Kass *et al*., 1989).

3. A More Detailed Analysis of the Mitochondrial Localization of Aequorin Probes

Given the targeting signal, chimeric protein mtAEQ is expected to be localized to the mitochondrial matrix. However, the immunofluorescence data (see above) indicated only a general mitochondrial localization of mtAEQ, and it was not possible to discriminate its exact localization within the organelle. To ensure that our $[Ca^{2+}]$ measurements were indeed due to changes in the mitochondrial matrix, we analyzed the effect of uncouplers on the $[Ca^{2+}]$ values generated by our chimeric probe. Since Ca^{2+} entry into the mitochondrial matrix is driven by the electrochemical gradient across the IMM, collapse of this gradient with an uncoupler should abolish the changes in $[Ca^{2+}]$ measured by our probe. Using FCCP, a compound that dissipates the proton gradient across the IMM, the response to the histamine stimulus was abolished, as shown in Fig. 7A. This confirms that mtAEQ is localized to the mitochondrial matrix and that calcium accumulation occurs via the known uptake mechanism (the Ca^{2+} uniporter). Similar results were obtained using RR which inhibits calcium channels. Since cells are not permeable to RR,

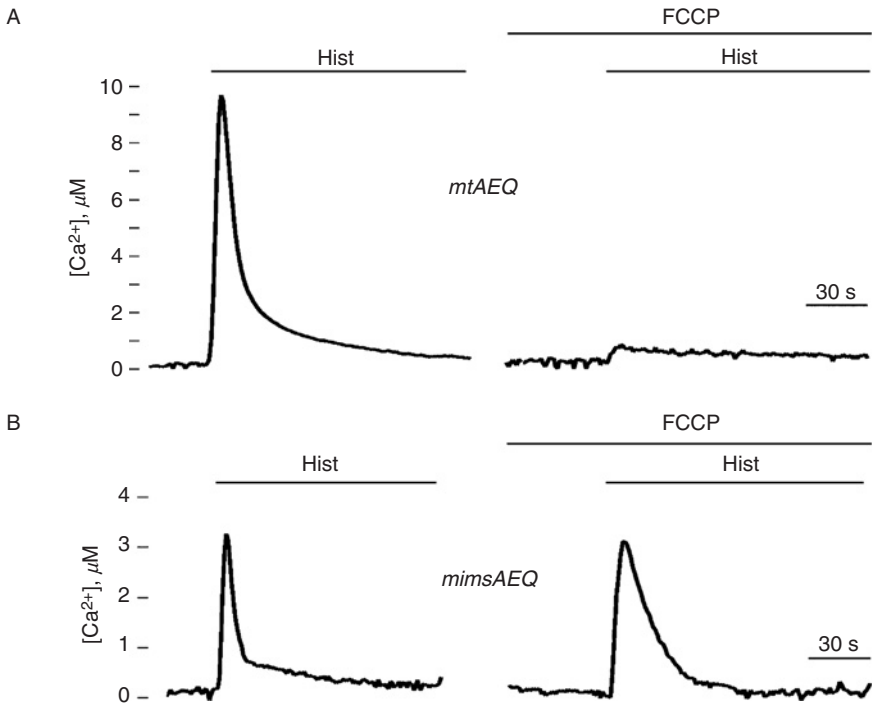

Fig. 7 Effect of FCCP on mitochondrial calcium measurements. (A) $[Ca^{2+}]_m$ changes on stimulation with histamine, in the absence and presence of FCCP (left and right panels, respectively). (B) $[Ca^{2+}]_{mims}$ changes on stimulation with histamine, in the absence and presence of FCCP (left and right panels, respectively).

cells were first permeabilized to all RR to gain access to the Ca^{2+} uniporter in mitochondria. Calcium uptake was then initiated by supplementing the medium with known concentrations of Ca^{2+}. On challenging with 2-μM free Ca^{2+}, $[Ca^{2+}]_m$ increased to over 3 μM, but in the presence of RR, uptake was almost completely abolished (data not shown).

To determine the exact location of mimsAEQ, we performed a similar series of experiments. As noted above, we had previously determined that the collapse of the proton gradient drastically reduces the accumulation of Ca^{2+} in the matrix, as visualized using mtAEQ. If mimsAEQ were mistargeted to the matrix, the rise in $[Ca^{2+}]$ should be abolished in the presence of uncouplers. Conversely, if mimsAEQ were localized in the intermembrane space, then the presence of uncouplers should not affect the $[Ca^{2+}]$ values obtained. As shown in Fig. 7B, HeLa cells transfected with mimsAEQ and treated with FCCP did not show a significant difference in $[Ca^{2+}]$ dynamics, when compared to similar, coupled cells, strongly suggesting that the aequorin moiety of mimsAEQ lies in the MIMS.

Taken as a whole, these experiments demonstrate that aequorin is useful as a calcium probe in a wide range of circumstances. Aequorin can be targeted to different subcellular locations (including different organelle compartments), where it can sense specific calcium changes (Chiesa *et al*., 2001). Moreover, the use of different mitochondrial drugs can be used to analyze calcium changes in a variety of conditions, as exemplified by, but not limited to, the cases documented above.

C. Mitochondrial Calcium Measurements Using GFP

In nature, GFP binds to aequorin (Chalfie, 1995; Chalfie *et al*., 1994; Rizzuto *et al*., 1996). Indeed, it is produced by the same jellyfish (*A. victoria*) and is situated in close association with the photoprotein, acting as a natural fluorophore that absorbs the blue light emitted by the aequorin and reemits photons of a longer wavelength (thus accounting for its own name and for the greenish hue of the jellyfish luminescence) (Ormo *et al*., 1996). In research applications, GFP retains its fluorescence properties, and thus can be added to the long list of probes in the cell biologist's toolbox. Some of its unique properties account for its explosive success, and has made it a powerful and versatile tool for investigating virtually all fields of cell biology, ranging from the study of gene expression to protein sorting, organelle structure, and measurements of physiological parameters in living cells (Rizzuto *et al*., 1996; Zhang *et al*., 2002).

The main reason for the success of GFP is its own nature: the fluorescent moiety is a gene product (with no need for cofactors) that is open to molecular engineering and transient or stable expression in virtually every cell type. Moreover, its mutagenesis has allowed for the adaptation of its fluorescence properties to different experimental needs (for a detailed description see the review by Zhang *et al*., 2002). Equally important, with the notable exception of the blue mutant, GFP is strongly resistant to photobleaching. As a result, it can be used for

applications including prolonged laser illumination during confocal microscopy. For these reasons, GFP has replaced available probes for many applications.

GFPs can also be used as sensors for physiological parameters. To overcome the problems of single cell-imaging experiments using aequorin probes, researchers have tried to exploit GFP to measure intracellular [Ca^{2+}]. Different Ca^{2+} indicators have been developed, by fusing of one or two GFP derivatives with a Ca^{2+}-binding protein, such as calmodulin (CaM) and/or a CaM-binding peptide. These chimeric probes are called cameleons, camgaroos, and pericams (Filippin *et al.*, 2005; Rudolf *et al.*, 2003; Zhang *et al.*, 2002). In general, these indicators can be classified depending on the process that causes the calcium signal. Cameleons are based on a fluorescent resonance energy transfer (FRET) process between two variants of GFP. Camgaroos and pericams can be classified as environment-sensitive GFPs. There are also fusion proteins (fusion aequorin-GFP and aequorin-RFP [red fluorescent protein]) that exhibit chemiluminescence resonance energy transfer (CRET or BRET) on binding calcium to aequorin.

1. Cameleons

FRET occurs only if the fluorescence emission spectrum of the ''donor'' GFP overlaps with the excitation spectrum of the ''acceptor'' GFP, and if the two fluorophores are located within few nanometers of each other and in a favorable orientation. Any alterations of these parameters can drastically alter the efficiency of FRET. Indeed, the rate of energy transfer is proportional to the sixth power of the distance $E = [1 + (R\backslash R_0)^6]^{-1}$, where R/R_0 is the fractional change in distance, and thus becomes negligible when the two fluorophores are >5–6 nm apart. The earliest use of FRET between GFP mutants was reported by Heim and Tsien (1996), who linked two fluorophores via a sequence of 25 amino acids, including a trypsin cleavage site. After addition of trypsin, the short peptide was cleaved and FRET was reduced drastically.

Cameleons are genetically encoded fluorescent indicators for Ca^{2+} based on chimeric proteins composed of four domains: a blue (BFP) or cyan (CFP) variant of GFP (the FRET donor), CaM, a glycylglycine linker, the CaM-binding domain of myosin light chain kinase (M13), and a green (GFP) or yellow (YFP) version of GFP (the FRET acceptor) (Miyawaki *et al.*, 1997, 1999). Modifications to improve and/or modulate their response have been performed in the GFP units and also in the calcium switch; as a result, different cameleons have been developed.

Cameleons change their structure on Ca^{2+} binding. The fluorescent proteins joined at both ends stand away from each other in the absence of calcium ion, and under these conditions thus excitation of CFP yields light emission mostly from CFP itself. This conformation has very low FRET probability. However, in the presence of calcium ion, the activated CaM wraps around the M13 protein. The structure of Cameleon then changes and reduces the distance between CFP and YFP. This conformational chkange makes CFP and YFP come together, and both

units adopt an orientation that induces an increase in FRET (FRET depends on distance between donor and acceptor and also on their relative orientation).

Yellow cameleons (YCs) are improved versions of cameleons composed of enhanced CFPs and YFPs. These constructs are more efficient than the original one, composed of BFP and GFP. BFP bleaches quickly, has a very low quantum yield, and requires UV excitation (excitation at ~430 nm), which might be cytotoxic and should be avoided. Conversely, YCs are brighter, more robust, and are excited by illumination that is less damaging.

YCs are classified in different groups, depending on their binding domains. Those in the YC2 group contain an intact CaM with high affinity for Ca^{2+}, while YC3 and YC4 have a mutation in CaM that lowers its affinity for calcium. For this reason, YC2 cameleons are high-affinity indicators ($K_d \sim 1.2\ \mu M$) and YC3 and YC4 are low-affinity indicators ($K_d \sim 4\ \mu M$ and $K_d \sim 105\ \mu M$, respectively). Different modifications in the YFP have been introduced to improve the properties of YCs. The original YCs were named as YC2, YC3, and YC4. Their first variants, YC2.1 and YC3.1, contain a mutation on YFP that decreases its sensitivity to acidification (rendering the signal unaffected at pH $\geq$ 6.5). Other mutations introduced into YFP allow for quicker maturation (Venus is a brighter version of YFP) or improve the cameleon's dynamic range.

The main drawback of most YCs is their poor dynamic range: the maximum variation between R_{max} and R_{min} obtained with YC3.12 is about 20%. However, the latest reported variant, YC3.60 (Nagai *et al*., 2004), has a promising dynamic range of nearly 600% which dramatically improves signal-to-noise ratio.

Cameleons are used as ratiometric indicators to increase the signal-to-noise ratio (in the case of the CFP–YFP pair, emission is measured at 480 and 535 nm). An example of mitochondrial [Ca^{2+}] measurements using targeted cameleons is shown in Fig. 8A.

2. Camgaroos and Pericams

Camgaroos and pericams are based on the fact that GFP and its mutants do not lose their ability to fold and form the chromophore if they are modified at tyrosine-145. This allows insertion of peptides between positions 145 and 146, and is the origin of camgaroos and pericams. In the case of camgaroos (Fig. 8B), a CaM unit is bound to positions 145 and 146 of YFP. When calcium interacts with CaM, the protein changes its conformation and induces an increase in fluorescence of YFP.

Pericams (Fig. 8C) are obtained by a more complex approach; the linear sequence of YFP is cleaved between positions 145 and 146 (generating new C and N termini at the cleavage site), while the original C and N termini are fused. This modification is called circular permutation. The linkage of CaM and CaM-binding domain of myosin light chain kinase (M13) to the new C and N termini makes pericams sensitive to calcium. Three types of pericams have been developed by mutating several amino acids adjacent to the chromophore.

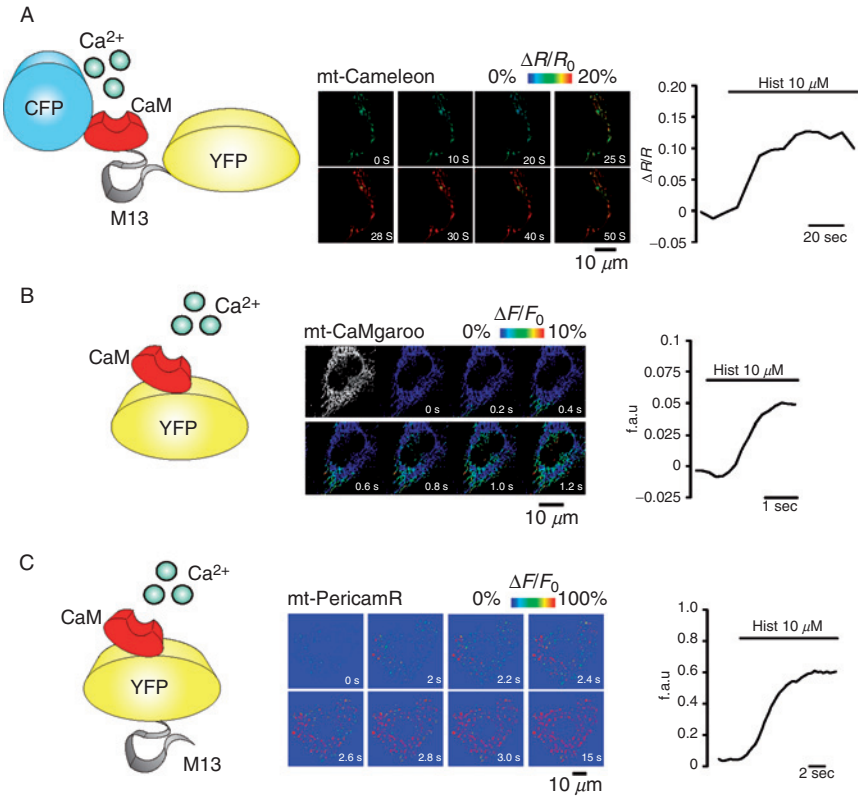

Fig. 8 Camgaroos and pericams. (A) [Ca^{2+}] measurement using mtCaMgaroo-2. On the *left*, the schematic structure of CaMgaroo is shown. On the *right* the pseudocolor-rendered images of ratio values (F/F_0) show the changes in fluorescence after a 5-sec puff of histamine (10 μM). At each time point (200 msec apart), the [Ca^{2+}] is measured in mitochondria. The trace representing the changes in fluorescence (f.a.u., fluorescence arbitrary units) of $[Ca^{2+}]_m$ during histamine challenge. (B) [Ca^{2+}] measurement using mtPericamR. On the *left*, the schematic structure of mitochondrial ratiometric-pericam is shown; on the *right* is a representative experiment. The cells were illuminated at 410 nm at 100-msec intervals. The pseudocolor images show the changes in fluorescence after stimulation with 10-μM histamine. Ca^{2+} concentrations are color coded, with a basal Ca^{2+} concentration in blue and a high Ca^{2+} concentration in red. The *black trace* represents the kinetic changes of the $\Delta F/F_0$ ratio over large mitochondrial region of a single representative cell. (C) Mitochondrial calcium response measurement using mtYC2.1. On the *left*, the schematic structure of mitochondrial targeting Cameleon (mtYC 2.1) is shown; on the *right* is a representative experiment. Emission ratio images were obtained at 440 nm excitation and 510/20 nm (YFP) and 460/20 nm (CFP) emission, and are rendered in pseudocolor. The normalized trace represents the $[Ca^{2+}]_m$ change in HeLa cells stimulated with 100-μM histamine.

Of these, "flash-pericam" became brighter with Ca^{2+}, whereas "inverse-pericam" became dimmer. On the other hand, "ratiometric-pericam" had an excitation wavelength that changed in a Ca^{2+}-dependent manner (Nagai *et al.*, 2001).

Compared with cameleons, pericams show greater Ca^{2+} responses and improved signal-to-noise ratio (Nagai *et al.*, 2001). By contrast to low Ca^{2+}-affinity camgaroos ($K_d = 7$ μmol/l) (Baird *et al.*, 1999), pericams have higher Ca^{2+} affinity ($K_d = 0.7$ μmol/l), which is favorable for sensing physiological Ca^{2+} changes.

Both kind of indicators are usually employed in nonratiometric measurements and are affected by changes in pH. An example of mitochondrial [Ca^{2+}] measurements using targeted camgaroos and pericams is reported in Fig. 8B and C, respectively.

Figure 9 shows an example of the use of those probes for high-speed single cell imaging of mitochondrial Ca^{2+} changes simultaneously with cytosolic measurements

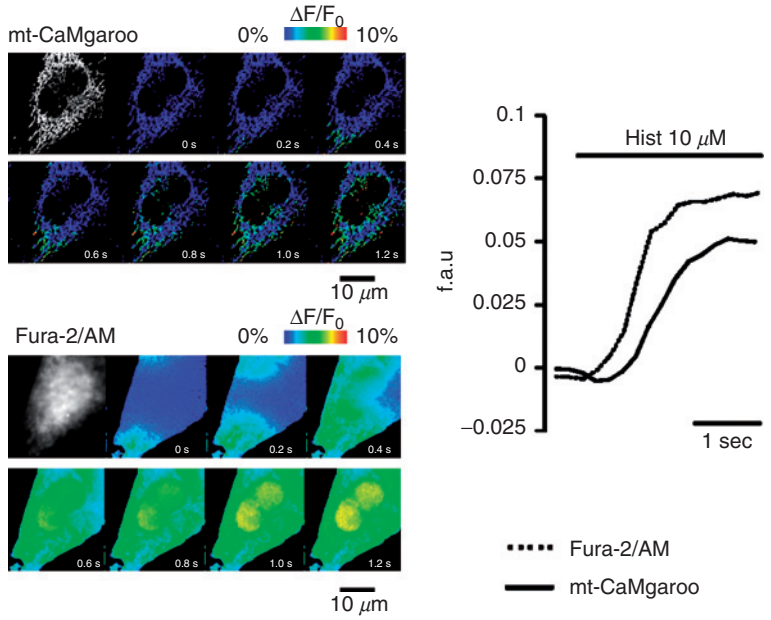

Fig. 9 Simultaneous single cell imaging of mitochondrial and cytosolic [Ca^{2+}] changes in single cell. The imaging of Fura-2/AM (bottom) and mt-CaMgaroo (top) is shown. The black and white images show Fura-2/AM and three-dimensional CaMgaroo distribution within the cells. The pseudocolored images (350 nm/380 nm ratio for Fura-2/AM and 514 excitation for CaMgaroo) show the changes in fluorescence after a 5-sec puff of histamine (Hist 10 μM). At each time point (200 msec apart), the [Ca^{2+}] is measured simultaneously in the cytosol and mitochondria. On the right, the traces representing the changes in fluorescence (f.a.u., fluorescence arbitrary units) of $[Ca^{2+}]_c$ (dotted lines) and $[Ca^{2+}]_m$ (continuous lines) are shown.

(using an organelle-targeted camgaroo for the mitochondria and the Fura-2 for the cytosol). The results demonstrated that the $[Ca^{2+}]_c$ rise evoked by cell stimulation is followed by a delayed upstroke of $[Ca^{2+}]_m$ (Rapizzi *et al.*, 2002).

D. Procedure

Cells grown on 24-mm diameter coverslips are transfected with 8 μg of DNA bearing the GFP-based sensor of interest. After 36 h, the coverslip is placed on a thermostatted chamber in KRB saline solution and $[Ca^{2+}]$ changes are determined using a high-speed, wide-field digital-imaging microscope. A microperfusion system (ALA DVD-12, Ala Scientific, NY), allowing rapid solution exchange, can be used to apply stimuli. Perfusion and image acquisition are controlled by MetaFluor 5.0 software (Universal Imaging Corporation, PA).

The emission ratio of cameleon (excitation wavelength of 430 nm and emission at 480 and 535 nm) is acquired at 2 frames per second using a CoolSNAPHQ interline CCD camera (Roper Scientific, NJ) using a 440/20-nm excitation filter, 455DCLP dichroic, and 485/40-nm or 535/30-nm emission filters (Chroma Technology, VT) placed in an emission filter wheel controlled by Lambda 10–2 (Sutter Instrument, Novato, CA). For fast kinetic imaging of $[Ca^{2+}]_m$, the probe is excited at 410 nm, using a random access monochromator (Photon Technology International, NJ). Images are acquired at 5–10 frames per second using a BFT512 back-illuminated camera (Princeton Instruments, AZ). Dual-excitation imaging with ratiometric pericam or camgaroo (two excitation wavelengths at 415 and 490 nm, and emission at 525 nm) use two excitation filters (480DF10 and 410DF10), which are alternated by a filter changer (Lambda 10–2, Sutter Instruments), a 505 DRLP-XR dichroic mirror, and a 535DF25 emission filter (Rizzuto *et al.*, 1998a).

IV. pH Reporters

All cells contain an intracellular fluid with a defined and highly controlled pH value—this is known as the intracellular pH (pHi). The pHi plays a critical role in cellular function, and tight regulation of pH is required for cell survival. There are numerous mechanisms that can cause pHi to change, including metabolic acid production, leakage of acid across plasma and organelle membranes, and membrane transport processes. pHi regulates many cellular processes, including cell metabolism (Roos and Boron, 1981), gene expression (Isfort *et al.*, 1993, 1996), cell–cell coupling (Orchard and Kentish, 1990), and cell death (Gottlieb *et al.*, 1996).

In mitochondria, it is universally accepted that the H^+ electrochemical potential ($\Delta\mu_{H^+}$), generated by electron transport across the inner membrane coupled to H^+ ejection on the redox H^+ pumps, is used to drive ATP synthesis by the F_oF_1-ATP synthase. In addition to ATP synthesis, $\Delta\mu_{H^+}$ supports a variety of mitochondrial processes, some of which are a prerequisite for respiration and ATP synthesis,

such as the uptake of respiratory substrates and phosphate, the uptake of ADP in exchange for ATP and of Ca^{2+} ions, the transhydrogenation reaction, and the import of respiratory chain and ATP synthase subunits encoded by nuclear genes. $\Delta\mu_{H^+}$ comprises both the electrical ($\Delta\psi$) and the chemical component of the H^+ gradient (ΔpH). It is well established that under physiological conditions, $\Delta\psi$ represents the dominant component of $\Delta\mu_{H^+}$, whereas the ΔpH gradient is small. The relative contribution of $\Delta\psi$ and ΔpH across the mitochondrial membrane can be changed by the redistribution of permeant ions, such as phosphate, Ca^{2+}, or K^+, in the presence of the ionophore valinomycin. Several techniques have been developed for the determination of $\Delta\psi$ and ΔpH in isolated mitochondria. Attempts have been also made to measure $\Delta\psi_m$ in intact cells (for a critical evaluation of these methods, see Bernardi *et al.*, 1999). However, measurements of matrix pH have been elusive, due to the difficulty of separating the mitochondrial signal from that in the surrounding cytoplasm (Chacon *et al.*, 1994). One of the most promising tools developed to overcome this difficulty the use of recombinant pH-sensitive fluorescent proteins targeted specifically to the mitochondrial compartments.

A. Mitochondrial pH-Sensitive Fluorescent Proteins

The pH sensitivity of GFP, and in particular of some of its mutants, is usually a disadvantage, confounding the interpretation of other data (e.g., FRET-based measurements of $[Ca^{2+}]$). In the case of the measurement of pH, however, this disadvantage can be turned to an advantage. Both purified and recombinant wild-type GFP, and most of the GFP mutants, are influenced by pH, suggesting that pHi sensitivity is a general property of this entire class of proteins (Patterson *et al.*, 1997; Ward and Bokman, 1982). Early after the first reports on the use of GFP as a general reporter, GFP mutants appeared promising as pH sensors in living cells. This possibility was first investigated by Kneen *et al.* (1998), who reported that mutations S65T and F64L/S65T in wild-type GFP exhibited fluorescent spectra and pH titration data indistinguishable from the unmutated polypeptide, with a pK_a value of 5.98. In addition, the finding that the titration curve for GFP-S65T was similar to that of fluorescein suggested the involvement of only a single amino acid residue in its pH-sensitive mechanism (Kneen *et al.*, 1998). Crystallographic analysis of this GFP mutant at both basic (pH 8.0) and acidic (pH 4.6) pH identified a model, likely valid for other mutants as well, where the phenolic hydroxyl of Tyr-66 is the site of protonation (Elsliger *et al.*, 1999).

The same GFP mutant (F64L/S65T), termed GFPmut1, was expressed heterologously in the cytosol and nuclear compartments of BS-C-1 rabbit proximal tubule cells. In this study, comparison of GFPmut1 with the pH-sensitive dye BCECF fluorescence showed a uniform agreement between pHi estimates using the two methods (Robey *et al.*, 1998).

Another pH-sensitive GFP mutant, named enhanced yellow fluorescent protein (EYFP), was made by introducing the amino acid substitutions S65G/S72A/T203Y. The absorbance spectrum of EYFP *in vitro* (Fig. 10A) shows that the

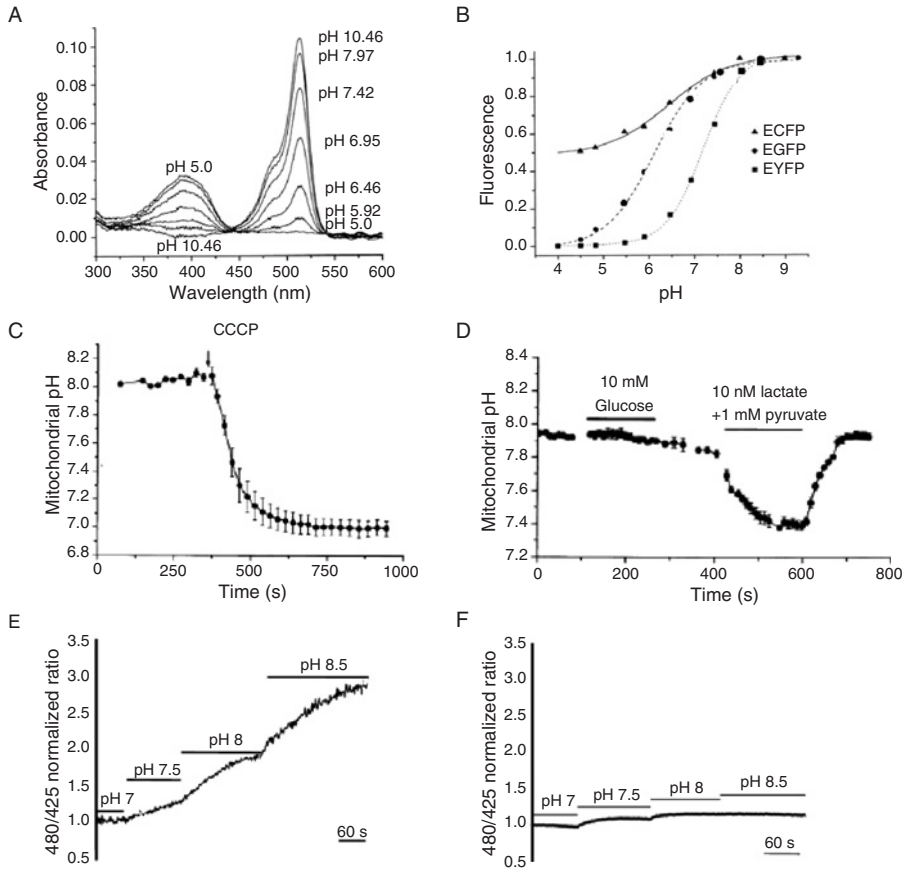

Fig. 10 pH reporters. (A) pH-dependent absorbance of EYFP (modified from Llopis *et al.*, 1998). (B) pH dependency of fluorescence of various GFP mutants. The fluorescence intensity of purified recombinant GFP mutant protein as a function of pH was measured in a microplate fluorometer (modified from Llopis *et al.*, 1998). (C) The uncoupler CCCP collapses mitochondrial pH (modified from Llopis *et al.*, 1998). (D) Effect of glucose and lactate/pyruvate perfusion on mitochondrial pH (modified from Llopis *et al.*, 1998). (E and F) HeLa cells coexpressing mtAlpHi and mtECFP were perfused with mKRB, supplemented with the ionophores nigericin and monensin (5 μM). The pH was increased in 0.5-unit steps, from 7.0 to 8.5, and the fluorescence of both probes was monitored. For comparison, HeLa cells coexpressing mtEYFP and mtECFP were subjected to the same protocol. Whereas mtAlpHi yields a signal that increases by threefold between pH 7 and 8.5, mtEYFP shows an increase of only <15% (modified from Abad *et al.*, 2004).

absorbance of the peak at 514 nm increased from pH 5–8 (Llopis *et al.*, 1998). The apparent pK_a (pK'_a) of EYFP is 7.1, compared to a pK'_a of EGFP of 6.15. The change in fluorescence of enhanced cyan fluorescent protein (ECFP) with pH (pK'_a, 6.4) is smaller than that of EGFP or EYFP (Fig. 10B).

The suitability of these GFP mutants as pH indicators in the mitochondrial matrix of living cells was evaluated in CHO (Kneen *et al*., 1998), HeLa cells, and in rat neonatal cardiomyocytes (Llopis *et al*., 1998). In CHO cells expressing recombinant GFPmut1 targeted to the mitochondrial matrix, a qualitative reversible acidification of mitochondria was observed after addition of the protonophore CCCP. However, the pH value of the mitochondrial matrix could not be determined accurately due to the low pK_a of this GFP mutant. Thus, GFP-mut1 is not a suitable pH indicator in this compartment, but it would be advantageous in more acidic organelles, such as the cytoplasm and trans-Golgi cisternae (Kneen *et al*., 1998). Conversely, expression of EYFP allowed for the quantitative determination of pH changes in the mitochondrial matrix. The resting value, which was 7.98 in HeLa cells and 7.91 in rat neonatal cardiomyocytes, collapsed rapidly to about pH 7 following addition of a protonophore (Fig. 10C), indicating that this GFP mutant is a good tool for measurement of mitochondrial matrix pH (Llopis *et al*., 1998).

In resting cells, the matrix pH did not change following addition of medium containing 10-mM glucose (an oxidizable substrate), but growth in medium containing 10-mM lactate plus 1-mM pyruvate caused an acidification (Fig. 10D), which was reversible on washout. This can be accounted for by diffusion of the protonated acid or by cotransport of $pyruvate^-/H^+$ through the IMM (Llopis *et al*., 1998).

A new GFP-based pH indicator with a pK'_a in the alkaline region (i.e., with an ideal sensitivity to monitor pH variations within the mitochondrial matrix), named mtAlpHi, for mitochondrial alkaline pH indicator, has been developed (Abad *et al*., 2004). This probe appears even more suitable than mtEYFP for studying the pH dynamics of mitochondrial matrix; it responds rapidly and reversibly to changes in pH, it has a pK'_a around 8.5, and it lacks toxicity or evident interference with normal cellular functions. Moreover the dynamic range of mtAlpHi fluorescence is markedly different from that of mtEYFP, whereas the former increases approximately threefold between pH 7 and 8.5, the latter shows a much smaller change (<15%) (Fig. 10E and F). With mtAlpHi, it has been calculated that the mitochondrial matrix pH in intact cells in steady state conditions is 8.05 ± 0.11, and on addition of FCCP this value drops to about 7.50 ± 0.22.

An equally important compartment is the intermembrane space of mitochondria, that is, the other side of the membrane across which the respiratory chain pumps H^+. Given the much smaller volume (compensated by the diffusion to the cytosol through the OMM) pH values could significantly differ from those of the neighboring regions. To get insight into this important bioenergetic parameter, we developed a specific YFP-based pH sensor. For this purpose, the same cloning strategy employed for mimsAEQ (Pinton *et al*., 1998; Rizzuto *et al*., 1998b) was followed, and mimsYFP was generated (Porcelli *et al*., 2005). When transfected in HeLa cells, mimsYFP showed a classical mitochondrial distribution (i.e., typical rod-like structures distributed throughout the cytoplasm). The choice of a GFP mutant with a pK_a value around 7 as a suitable pH sensor in this compartment

derives from the assumption that the pH of the MIMS is in equilibrium with that of cytosol. Indeed, the outer membrane has not been considered a barrier to transport of ions and molecules up to 5 kDa (Mannella *et al.*, 1998). However, the MIMS might be influenced by pH changes occurring in the matrix as a result of variations of the $\Delta\psi$, and microdomains exhibiting different $[H^+]$ from cytosol might exist under physiological and pathological conditions.

In order to generate a titration curve of mimsYFP, we quantitated the fluorescence of mimsEYFP as a function of pH (Fig. 11A). Coverslips with mimsEYFP-transfected cells were mounted in the thermostatted chamber (37°C) of a digital-imaging system, and were incubated in a KCl-based saline solution containing 125-mM KCl, 20-mM NaCl, 5.5-mM D-glucose, 1-mM $CaCl_2$, 1-mM $MgSO_4$, 1-mM K_2HPO_4, 20-mM Na-HEPES (pH 6.5), and the ionophores nigericin plus monensin (5 μM each) to equilibrate intracellular and extracellular pH. pH was increased by the addition of small amounts of NaOH while measuring the pH with a semimicro-combination pH electrode. Fluorescence of mimsEYFP in selected areas of cells was linear with respect to pH over the range between pH 6.5 and 8. When the average values of fluorescence in the selected areas were plotted against pH, we obtained the calibration curve shown in Fig. 11B (Porcelli *et al.*, 2005).

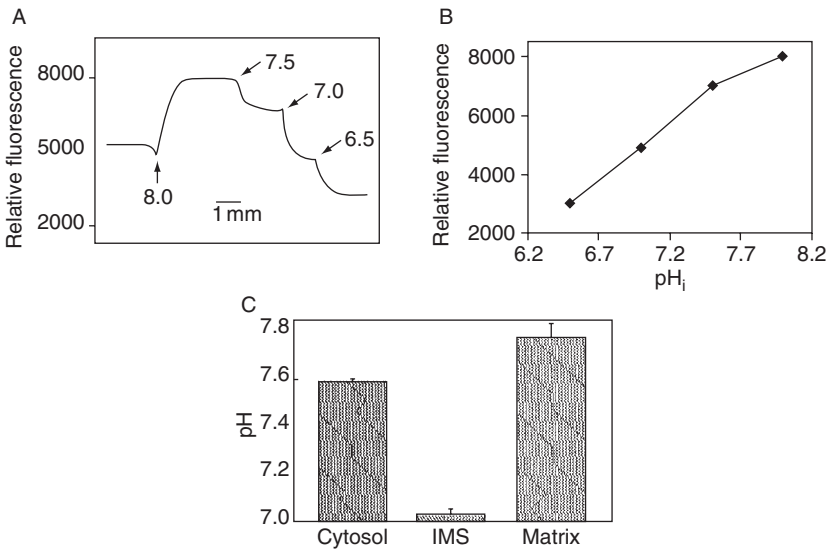

Fig. 11 pH measurements in mitochondria. (A) MIMS-EYFP-transfected ECV304 cells were first incubated with KBS, then perfused with high KCl saline solution containing nigericin and monensin (5 μM) at the indicated pH, as detailed in the figure (modified from Porcelli *et al.*, 2005). (B) Normalized values of fluorescence intensity obtained in (A) are plotted against pH. Data are means ± SD (modified from Porcelli *et al.*, 2005). (C) Values of pH in the cytosol, MIMS, and mitochondrial matrix. ECV304 cells were transfected with cytosolic EYFP, mimsEYFP, or mtEYFP, incubated with KBS, and then perfused as described in (A) (modified from Porcelli *et al.*, 2005).

Using the mimsYFP, mtYFP, and cytYFP probes with this calibration curve, the following pH values were obtained: MIMS 6.88 ± 0.09; mitochondrial matrix 7.78 ± 0.17, and cytosol 7.59 ± 0.01 (Fig. 11C) (Porcelli *et al*., 2005).

B. Procedure

The procedures employed for expressing mtYFP and mimsYFP are the same as those described previously for the corresponding aequorin chimeras, that is, in most cases, transection can be accomplished by a simple transfection with the calcium phosphate protocol. The only difference is that the cells are seeded onto 24-mm coverslips and are transfected with 8-μg DNA/coverslip. In the case of mimsYFP, the amount of DNA can be reduced to 2–4 μg per coverslip to prevent mitochondrial damage. It is our experience that in many cell types high levels of expression of a recombinant protein retained in the intermembrane space (i.e., not only YFP, but also aequorin, see above) cause a change in the morphology of mitochondria. After 36 h of transfection, the coverslip is transferred to the thermostatted stage of a digital-imaging system, as described previously for the GFP-based calcium probes. For YFP chimeras, dedicated YFP filter sets (500/542 nm) are usually used, but comparable results can also be obtained with a traditional FITC set (482/536 nm). For mtAlpHi, the maximal peak is at 498 nm for the excitation and 522 nm for the emission light.

V. Conclusions

Genetically encoded biosensors (chimeric proteins) are intracellular probes of physiological parameters endowed with unique advantages. These advantages include the ability to measure intracellular parameters (such as Ca^{2+} and pH) at specific intracellular sites, with little background signal, and no probe leakage. Additionally, the use of biosensors is not associated with the toxicity observed with many chemical probes nor with the need of invasive loading procedures. Furthermore, an ideal intracellular probe should be stable, have high parameter sensitivity and specificity, rapid signal response to parameter changes, and good luminescent/optical properties. The probes described here fulfill many of these requirements.

Acknowledgments

The authors are deeply indebted to past and present collaborators. We thank the Italian University Ministry (MURST), Telethon-Italy (Grants no. GGP05284 and GTF02013), the Italian Association for Cancer Research (AIRC), the Italian Space Agency (ASI), EU (fondi strutturali Obiettivo 2), and the PRRIITT program of the Emilia Romagna Region for financial support.

References

Abad, M. F., Di Benedetto, G., Magalhaes, P. J., Filippin, L., and Pozzan, T. (2004). Mitochondrial pH monitored by a new engineered green fluorescent protein mutant. *J. Biol. Chem.* **279,** 11521–11529.

Allen, D. G., and Blinks, J. R. (1978). Calcium transients in aequorin-injected frog cardiac muscle. *Nature* **273,** 509–513.

Baird, G. S., Zacharias, D. A., and Tsien, R. Y. (1999). Circular permutation and receptor insertion within green fluorescent proteins. *Proc. Natl. Acad. Sci. USA* **96,** 11241–11246.

Bastianutto, C., Clementi, E., Codazzi, F., Podini, P., De Giorgi, F., Rizzuto, R., Meldolesi, J., and Pozzan, T. (1995). Overexpression of calreticulin increases the Ca2+ capacity of rapidly exchanging Ca2+ stores and reveals aspects of their lumenal microenvironment and function. *J. Cell Biol.* **130,** 847–855.

Bernardi, P. (1999). Mitochondrial transport of cations: Channels, exchangers, and permeability transition. *Physiol. Rev.* **79,** 1127–1155.

Bernardi, P., Scorrano, L., Colonna, R., Petronilli, V., and Di Lisa, F. (1999). Mitochondria and cell death. Mechanistic aspects and methodological issues. *Eur. J. Biochem.* **264,** 687–701.

Berridge, M. J., Lipp, P., and Bootman, M. D. (2000). The versatility and universality of calcium signalling. *Nat. Rev. Mol. Cell Biol.* **1,** 11–21.

Berridge, M. J., Bootman, M. D., and Roderick, H. L. (2003). Calcium signalling: Dynamics, homeostasis and remodelling. *Nat. Rev. Mol. Cell Biol.* **4,** 517–529.

Brini, M., Marsault, R., Bastianutto, C., Alvarez, J., Pozzan, T., and Rizzuto, R. (1995). Transfected aequorin in the measurement of cytosolic Ca2+ concentration ([Ca2+]c). A critical evaluation. *J. Biol. Chem.* **270,** 9896–9903.

Budd, S. L., and Nicholls, D. G. (1996a). A reevaluation of the role of mitochondria in neuronal Ca2+ homeostasis. *J. Neurochem.* **66,** 403–411.

Budd, S. L., and Nicholls, D. G. (1996b). Mitochondria, calcium regulation, and acute glutamate excitotoxicity in cultured cerebellar granule cells. *J. Neurochem.* **67,** 2282–2291.

Carafoli, E. (1987). Intracellular calcium homeostasis. *Annu. Rev. Biochem.* **56,** 395–433.

Chacon, E., Reece, J. M., Nieminen, A. L., Zahrebelski, G., Herman, B., and Lemasters, J. J. (1994). Distribution of electrical potential, pH, free Ca2+, and volume inside cultured adult rabbit cardiac myocytes during chemical hypoxia: A multiparameter digitized confocal microscopic study. *Biophys. J.* **66,** 942–952.

Chalfie, M. (1995). Green fluorescent protein. *Photochem. Photobiol.* **62,** 651–656.

Chalfie, M., Tu, Y., Euskirchen, G., Ward, W. W., and Prasher, D. C. (1994). Green fluorescent protein as a marker for gene expression. *Science* **263,** 802–805.

Chiesa, A., Rapizzi, E., Tosello, V., Pinton, P., de Virgilio, M., Fogarty, K. E., and Rizzuto, R. (2001). Recombinant aequorin and green fluorescent protein as valuable tools in the study of cell signalling. *Biochem. J.* **355,** 1–12.

Cobbold, P. H. (1980). Cytoplasmic free calcium and amoeboid movement. *Nature* **285,** 441–446.

De Giorgi, F., Brini, M., Bastianutto, C., Marsault, R., Montero, M., Pizzo, P., Rossi, R., and Rizzuto, R. (1996). Targeting aequorin and green fluorescent protein to intracellular organelles. *Gene* **173,** 113–117.

Drummond, R. M., and Fay, F. S. (1996). Mitochondria contribute to Ca2+ removal in smooth muscle cells. *Pflugers Arch.* **431,** 473–482.

Duchen, M. R. (1999). Contributions of mitochondria to animal physiology: From homeostatic sensor to calcium signalling and cell death. *J. Physiol.* **516**(Pt. 1), 1–17.

Duchen, M. R. (2000a). Mitochondria and Ca(2+) in cell physiology and pathophysiology. *Cell Calcium* **28,** 339–348.

Duchen, M. R. (2000b). Mitochondria and calcium: From cell signalling to cell death. *J. Physiol.* **529** (Pt. 1), 57–68.

Elsliger, M. A., Wachter, R. M., Hanson, G. T., Kallio, K., and Remington, S. J. (1999). Structural and spectral response of green fluorescent protein variants to changes in pH. *Biochemistry* **38,** 5296–5301.

Filippin, L., Abad, M. C., Gastaldello, S., Magalhaes, P. J., Sandona, D., and Pozzan, T. (2005). Improved strategies for the delivery of GFP-based Ca2+ sensors into the mitochondrial matrix. *Cell Calcium* **37,** 129–136.

Gavel, Y., and von Heijne, G. (1990). Cleavage-site motifs in mitochondrial targeting peptides. *Protein Eng.* **4,** 33–37.

Gottlieb, R. A., Gruol, D. L., Zhu, J. Y., and Engler, R. L. (1996). Preconditioning rabbit cardiomyocytes: Role of pH, vacuolar proton ATPase, and apoptosis. *J. Clin. Invest.* **97,** 2391–2398.

Green, D. R., and Kroemer, G. (2004). The pathophysiology of mitochondrial cell death. *Science* **305,** 626–629.

Gunter, K. K., and Gunter, T. E. (1994). Transport of calcium by mitochondria. *J. Bioenerg. Biomembr.* **26,** 471–485.

Gunter, T. E., Buntinas, L., Sparagna, G., Eliseev, R., and Gunter, K. (2000). Mitochondrial calcium transport: Mechanisms and functions. *Cell Calcium* **28,** 285–296.

Gunter, T. E., and Gunter, K. K. (2001). Uptake of calcium by mitochondria: Transport and possible function. *IUBMB Life* **52,** 197–204.

Hajnoczky, G., Robb-Gaspers, L. D., Seitz, M. B., and Thomas, A. P. (1995). Decoding of cytosolic calcium oscillations in the mitochondria. *Cell* **82,** 415–424.

Heim, R., and Tsien, R. Y. (1996). Engineering green fluorescent protein for improved brightness, longer wavelengths and fluorescence resonance energy transfer. *Curr. Biol.* **6,** 178–182.

Herrington, J., Park, Y. B., Babcock, D. F., and Hille, B. (1996). Dominant role of mitochondria in clearance of large Ca2+ loads from rat adrenal chromaffin cells. *Neuron* **16,** 219–228.

Isfort, R. J., Cody, D. B., Asquith, T. N., Ridder, G. M., Stuard, S. B., and LeBoeuf, R. A. (1993). Induction of protein phosphorylation, protein synthesis, immediate-early-gene expression and cellular proliferation by intracellular pH modulation. Implications for the role of hydrogen ions in signal transduction. *Eur. J. Biochem.* **213,** 349–357.

Isfort, R. J., Cody, D. B., Stuard, S. B., Ridder, G. M., and LeBoeuf, R. A. (1996). Calcium functions as a transcriptional and mitogenic repressor in Syrian hamster embryo cells: Roles of intracellular pH and calcium in controlling embryonic cell differentiation and proliferation. *Exp. Cell Res.* **226,** 363–371.

Jouaville, L. S., Pinton, P., Bastianutto, C., Rutter, G. A., and Rizzuto, R. (1999). Regulation of mitochondrial ATP synthesis by calcium: Evidence for a long-term metabolic priming. *Proc. Natl. Acad. Sci. USA* **96,** 13807–13812.

Kass, G. E., Duddy, S. K., Moore, G. A., and Orrenius, S. (1989). 1,2-Di-(tert-butyl)-1,4-benzohydroquinone rapidly elevates cytosolic Ca^{2+} concentration by mobilizing the inositol 1,4,5-trisphosphate-sensitive pool. *J. Biol. Chem.* **264,** 15192–15198.

Kendall, J. M., Sala-Newby, G., Ghalaut, V., Dormer, R. L., and Campbell, A. K. (1992). Engineering the CA(2+)-activated photoprotein aequorin with reduced affinity for calcium. *Biochem. Biophys. Res. Commun.* **187,** 1091–1097.

Kneen, M., Farinas, J., Li, Y., and Verkman, A. S. (1998). Green fluorescent protein as a noninvasive intracellular pH indicator. *Biophys. J.* **74,** 1591–1599.

Kroemer, G., and Reed, J. C. (2000). Mitochondrial control of cell death. *Nat. Med.* **6,** 513–519.

Lievremont, J. P., Rizzuto, R., Hendershot, L., and Meldolesi, J. (1997). BiP, a major chaperone protein of the endoplasmic reticulum lumen, plays a direct and important role in the storage of the rapidly exchanging pool of Ca2+. *J. Biol. Chem.* **272,** 30873–30879.

Llopis, J., McCaffery, J. M., Miyawaki, A., Farquhar, M. G., and Tsien, R. Y. (1998). Measurement of cytosolic, mitochondrial, and Golgi pH in single living cells with green fluorescent proteins. *Proc. Natl. Acad. Sci. USA* **95,** 6803–6808.

Mannella, C. A., Buttle, K., Rath, B. K., and Marko, M. (1998). Electron microscopic tomography of rat-liver mitochondria and their interaction with the endoplasmic reticulum. *Biofactors* **8,** 225–228.

Miyawaki, A., Llopis, J., Heim, R., McCaffery, J. M., Adams, J. A., Ikura, M., and Tsien, R. Y. (1997). Fluorescent indicators for Ca2+ based on green fluorescent proteins and calmodulin. *Nature* **388,** 882–887.

Miyawaki, A., Griesbeck, O., Heim, R., and Tsien, R. Y. (1999). Dynamic and quantitative Ca2+ measurements using improved cameleons. *Proc. Natl. Acad. Sci. USA* **96,** 2135–2140.

Montero, M., Brini, M., Marsault, R., Alvarez, J., Sitia, R., Pozzan, T., and Rizzuto, R. (1995). Monitoring dynamic changes in free Ca2+ concentration in the endoplasmic reticulum of intact cells. *EMBO J.* **14,** 5467–5475.

Montero, M., Barrero, M. J., and Alvarez, J. (1997). [Ca2+] microdomains control agonist-induced Ca2+ release in intact HeLa cells. *FASEB J.* **11,** 881–885.

Nagai, T., Sawano, A., Park, E. S., and Miyawaki, A. (2001). Circularly permuted green fluorescent proteins engineered to sense Ca2+. *Proc. Natl. Acad. Sci. USA* **98,** 3197–3202.

Nagai, T., Yamada, S., Tominaga, T., Ichikawa, M., and Miyawaki, A. (2004). Expanded dynamic range of fluorescent indicators for Ca(2+) by circularly permuted yellow fluorescent proteins. *Proc. Natl. Acad. Sci. USA* **101,** 10554–10559.

Nicholls, D. G. (2005). Mitochondria and calcium signaling. *Cell Calcium* **38,** 311–317.

Orchard, C. H., and Kentish, J. C. (1990). Effects of changes of pH on the contractile function of cardiac muscle. *Am. J. Physiol.* **258,** C967–C981.

Ormo, M., Cubitt, A. B., Kallio, K., Gross, L. A., Tsien, R. Y., and Remington, S. J. (1996). Crystal structure of the Aequorea victoria green fluorescent protein. *Science* **273,** 1392–1395.

Patterson, G. H., Knobel, S. M., Sharif, W. D., Kain, S. R., and Piston, D. W. (1997). Use of the green fluorescent protein and its mutants in quantitative fluorescence microscopy. *Biophys. J.* **73,** 2782–2790.

Pinton, P., Brini, M., Bastianutto, C., Tuft, R. A., Pozzan, T., and Rizzuto, R. (1998). New light on mitochondrial calcium. *Biofactors* **8,** 243–253.

Pinton, P., Ferrari, D., Magalhaes, P., Schulze-Osthoff, K., Di Virgilio, F., Pozzan, T., and Rizzuto, R. (2000). Reduced loading of intracellular Ca(2+) stores and downregulation of capacitative Ca(2+) influx in Bcl-2-overexpressing cells. *J. Cell Biol.* **148,** 857–862.

Porcelli, A. M., Ghelli, A., Zanna, C., Pinton, P., Rizzuto, R., and Rugolo, M. (2005). pH difference across the outer mitochondrial membrane measured with a green fluorescent protein mutant. *Biochem. Biophys. Res. Commun.* **326,** 799–804.

Pozzan, T., and Rizzuto, R. (2000). The renaissance of mitochondrial calcium transport. *Eur. J. Biochem.* **267,** 5269–5273.

Pozzan, T., Rizzuto, R., Volpe, P., and Meldolesi, J. (1994). Molecular and cellular physiology of intracellular calcium stores. *Physiol. Rev.* **74,** 595–636.

Rapizzi, E., Pinton, P., Szabadkai, G., Wieckowski, M. R., Vandecasteele, G., Baird, G., Tuft, R. A., Fogarty, K. E., and Rizzuto, R. (2002). Recombinant expression of the voltage-dependent anion channel enhances the transfer of Ca2+ microdomains to mitochondria. *J. Cell Biol.* **159,** 613–624.

Ridgway, E. B., and Ashley, C. C. (1967). Calcium transients in single muscle fibers. *Biochem. Biophys. Res. Commun.* **29,** 229–234.

Rizzuto, R., and Pozzan, T. (2006). Microdomains of intracellular Ca2+: Molecular determinants and functional consequences. *Physiol. Rev.* **86,** 369–408.

Rizzuto, R., Nakase, H., Darras, B., Francke, U., Fabrizi, G. M., Mengel, T., Walsh, F., Kadenbach, B., DiMauro, S., and Schon, E. A. (1989). A gene specifying subunit VIII of human cytochrome *c* oxidase is localized to chromosome 11 and is expressed in both muscle and non-muscle tissues. *J. Biol. Chem.* **264,** 10595–10600.

Rizzuto, R., Simpson, A. W., Brini, M., and Pozzan, T. (1992). Rapid changes of mitochondrial Ca2+ revealed by specifically targeted recombinant aequorin. *Nature* **358,** 325–327.

Rizzuto, R., Brini, M., Murgia, M., and Pozzan, T. (1993). Microdomains with high Ca2+ close to IP3-sensitive channels that are sensed by neighboring mitochondria. *Science* **262,** 744–747.

Rizzuto, R., Brini, M., De Giorgi, F., Rossi, R., Heim, R., Tsien, R. Y., and Pozzan, T. (1996). Double labelling of subcellular structures with organelle-targeted GFP mutants *in vivo*. *Curr. Biol.* **6,** 183–188.

Rizzuto, R., Carrington, W., and Tuft, R. A. (1998a). Digital imaging microscopy of living cells. *Trends Cell Biol.* **8,** 288–292.

Rizzuto, R., Pinton, P., Carrington, W., Fay, F. S., Fogarty, K. E., Lifshitz, L. M., Tuft, R. A., and Pozzan, T. (1998b). Close contacts with the endoplasmic reticulum as determinants of mitochondrial Ca2+ responses. *Science* **280,** 1763–1766.

Rizzuto, R., Bernardi, P., and Pozzan, T. (2000). Mitochondria as all-round players of the calcium game. *J. Physiol.* **529**(Pt. 1), 37–47.

Rizzuto, R., Duchen, M. R., and Pozzan, T. (2004). Flirting in little space: The ER/mitochondria Ca2+ liaison. *Sci. STKE* **2004**(215), re1.

Robey, R. B., Ruiz, O., Santos, A. V., Ma, J., Kear, F., Wang, L. J., Li, C. J., Bernardo, A. A., and Arruda, J. A. (1998). pH-dependent fluorescence of a heterologously expressed Aequorea green fluorescent protein mutant: *In situ* spectral characteristics and applicability to intracellular pH estimation. *Biochemistry* **37,** 9894–9901.

Roos, A., and Boron, W. F. (1981). Intracellular pH. *Physiol. Rev.* **61,** 296–434.

Rudolf, R., Mongillo, M., Rizzuto, R., and Pozzan, T. (2003). Looking forward to seeing calcium. *Nat. Rev. Mol. Cell Biol.* **4,** 579–586.

Rutter, G. A., Burnett, P., Rizzuto, R., Brini, M., Murgia, M., Pozzan, T., Tavare, J. M., and Denton, R. M. (1996). Subcellular imaging of intramitochondrial Ca2+ with recombinant targeted aequorin: Significance for the regulation of pyruvate dehydrogenase activity. *Proc. Natl. Acad. Sci. USA* **93,** 5489–5494.

Shimomura, O. (1986). Isolation and properties of various molecular forms of aequorin. *Biochem. J.* **234,** 271–277.

Shimomura, O., Johnson, F. H., and Saiga, Y. (1962). Extraction, purification and properties of aequorin, a bioluminescent protein from the luminous hydromedusan, Aequorea. *J. Cell. Comp. Physiol.* **59,** 223–239.

Ward, W. W., and Bokman, S. H. (1982). Reversible denaturation of Aequorea green-fluorescent protein: Physical separation and characterization of the renatured protein. *Biochemistry* **21,** 4535–4540.

Zhang, J., Campbell, R. E., Ting, A. Y., and Tsien, R. Y. (2002). Creating new fluorescent probes for cell biology. *Nat. Rev. Mol. Cell Biol.* **3,** 906–918.